

# Analysis of Spatiotemporal Patterns in a Model of Olfaction

Orit Kliper <sup>a,1</sup> David Horn <sup>b</sup> Brigitte Quenet <sup>c</sup> Gideon Dror <sup>d</sup>

<sup>a</sup>*School of Computer Sciences, Tel Aviv University, Tel Aviv 69978, Israel*

<sup>b</sup>*School of Physics and Astronomy, Tel Aviv University, Tel Aviv 69978, Israel*

<sup>c</sup>*Lab. d'Electronique, Ecole Supérieure de Physique et Chimie Industrielles, Paris 75005, France*

<sup>d</sup>*Department of Computer Science, The Academic College of Tel-Aviv-Yaffo, Tel Aviv 64044, Israel*

---

## Abstract

We model spatiotemporal patterns in Locust olfaction with the Dynamic Neural Filter (DNF), a recurrent network that produces spatiotemporal patterns in reaction to sets of constant inputs. We specify, within the model, inputs corresponding to different odors and different concentrations of the same odor. Then we proceed to analyze the resulting spatiotemporal patterns of the neurons of our model. Using SVD we investigate three kinds of data: global spatiotemporal data consisting of neuronal firing patterns over the period of odor presentation, spatial data, i.e. total spike counts during this period, and local spatiotemporal data which are neuronal spikes in single temporal bins.

*Key words:* Olfaction; Temporal Coding; Dynamic Neural Filter; Recurrent Network

---

## 1 Introduction

The Dynamic Neural Filter (DNF) (3) is a recurrent binary neural network that maps regions of input space into spatiotemporal sequences. It has been motivated by locust olfaction research. Here we take up the task of using this model as a prototype of spatiotemporal patterns, and put it to tests of the kind employed by (5) for data obtained from the locust antennal lobes (ALs).

---

<sup>1</sup> Corresponding author. e-mail: klipor@post.tau.ac.il

Since this kind of system is known to exhibit a local field potential (LFP) with temporal width of 50ms (6), we take this time window as the basic temporal bin in our discrete system, obeying

$$n_i(t+1) = H(h_i(t+1)) = H\left(\sum_j w_{ij}n_j(t) + R_i - \theta_i\right)$$

where  $n_i$  are the neural activity values,  $w_{ij}$  is the synaptic coupling matrix,  $R_i$  is an external input and  $\theta_i$  is the threshold.  $H$  is the Heaviside step function taking the values 0 for negative arguments and 1 for positive ones.

In the next section we define all other details of the model, after which we turn to a series of numerical experiments and their analysis.

## 2 Model of Olfaction

We use a fully connected binary network, defined by an asymmetric weight-matrix, with  $tr(\mathbf{w} \cdot \mathbf{w})/tr(\mathbf{w} \cdot \mathbf{w}^T) \approx 0$ , having both positive and negative couplings taken from a normal distribution of width 4. In a previous work (2) we discussed some features of the response sequences generated in large networks e.g.  $N = 40$ , by changing  $R$  values. We found that close-by  $R$  values generate divergent spatiotemporal sequences. We also found that the center of  $R$  space is the region where the system leads to large cycles and chaotic-like phenomena of total divergence occur. As we move out of the center of this space, small changes in  $R$  may lead to divergence, but finite correlations survive. These findings were consistent with the experimental results (1) in the olfactory bulb of Zebrafish. Fix points and short cycles appear mostly at the edges of the relevant  $R$  space, as defined in (3) and are not relevant to the current olfaction model. Let us limit ourselves to the ‘active range’ of  $R$  space where almost all sequences are long. This range can be defined by the standard deviation of the distribution of  $h$ , over all neurons and all time steps, in response to input at the center of  $R$  space. Numerical simulations lead to an active range of 20 for  $N=100$ .

Turning to olfaction, we note that neural firing behavior similar to that of Projection Neurons (PNs) of the ALs is seen at the lower end of the active range. Hence this will be chosen as the  $R$  value specifying the non-odor background activity, with all  $\theta$  values set to 0. Furthermore, we note that (4) have demonstrated a logarithmic relationship between the inputs (odors) at different concentrations and the receptors’ response. Inspired by these findings, the DNF inputs (for neuron  $i$  and odor  $j$ ) are expressed in terms of the logarithms of concentration, denoted by  $L$ , and are mapped onto the lower end of

the active range of  $R$  in the following way:

$$R_{ij} = m_i + s_{ij} \times L_j \times H(L_j - t_{ij})$$

where  $m_i$  is the starting point at the edge of the active range of  $R_i$ ,  $L_j$  is chosen from the set [1 2 3 4 5], and  $s_{ij}$  are randomly chosen from the interval [0.1-6].  $t_{ij}$  are the sensitivity thresholds, randomly chosen from the interval [0-15]. Neurons with  $t_{ij}$  above the highest concentrations will not be sensitive to the odor at all. Noise is added to the input values to represent stochastic fluctuations.

This model is supposed to represent the antennal lobe of locust. Although no attempt was made to distinguish between excitatory and inhibitory cells, or to follow other anatomical and physiological elements of the biological system, it may serve as a rudimentary model of the spatiotemporal behavior observed in this system. In particular, it allows us to investigate some interesting questions following from the analysis of such systems, comparing results of our model with those revealed in experiments (5).

### 3 Analysis of the spatiotemporal data

Similar to the work of (5) the data we analyzed were spatiotemporal patterns of 100 neurons over a simulation time of 1 sec. Figure 1 depicts such patterns, derived from a network of 100 neurons, all of which received a constant odor during a simulation of 20 time steps. Each of the frames, representing five concentrations of the three different odors, will be referred to as a ‘spatiotemporal pattern’. We proceed then to ask for clustering properties of such patterns for different odors and different concentrations. We choose SVD as our tool for dimensionality reduction. It is applied to the set of all data.

#### 3.1 Global Spatiotemporal Analysis

For each odor and concentration we generate 15 data points, differing from one another by noise. Thus we have 225 data points (15 points for each of 3 odors and 5 concentrations) each having a 2000 dimensional (100 neurons and 20 time bins) spatiotemporal pattern. SVD is applied to this 225×2000 matrix, truncating it down to 3 dimensions (corresponding to the three leading variance-eigenvalues). The 225 points may now be represented on these three dimensions. An example is presented in figure 2. Clusters of both odor and concentration exist. Thus we conclude that the global spatiotemporal patterns include this information, and it can be easily retrieved via SVD.

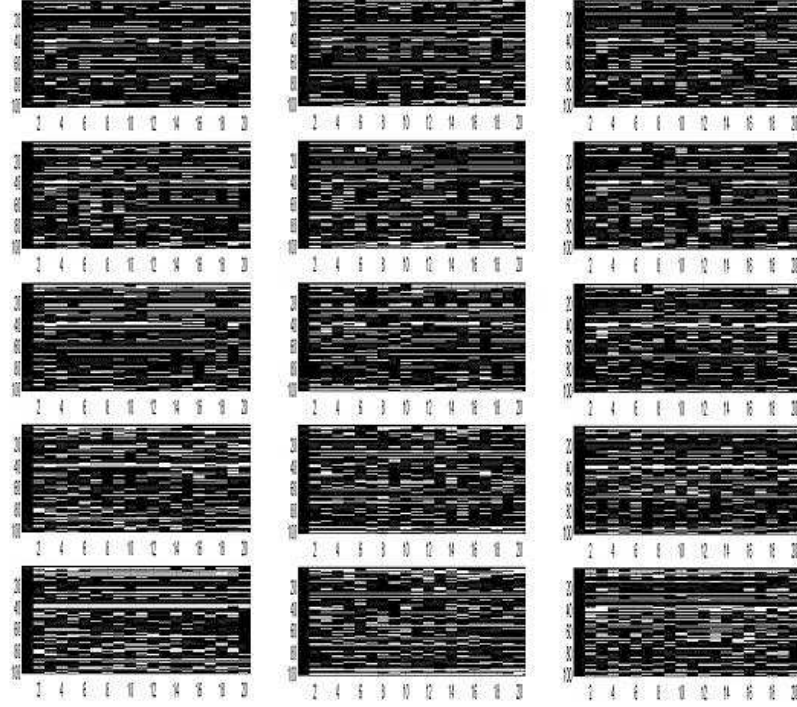


Fig. 1: Spatiotemporal patterns of three different odors, five concentrations each. Plots of an example trial are shown. (1 sec simulation in a network of 100 neurons. Noise with variance 0.01 was added to the inputs).

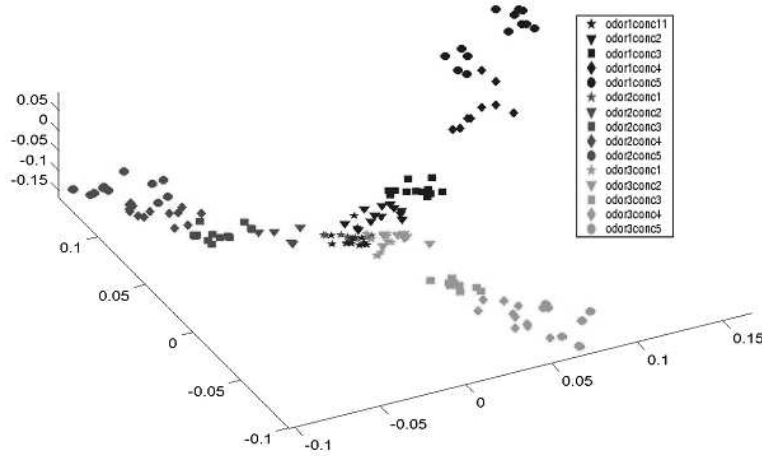


Fig. 2: Clustering of odors and concentrations observed in a 3-dimensional truncated SVD representation of the spatiotemporal patterns. Different shades represent different odors, while shapes represent concentrations.

### 3.2 Local Spatiotemporal Analysis

Next we ask ourselves if this type of information exists already at the level of single temporal bins, i.e. the columns of the spatiotemporal patterns discussed above. To answer this question we apply SVD to a matrix of  $4500 \times 100$ , cor-

responding to  $225 \times 20$  data-points (including the specific temporal bins) and 100 neural spatial patterns. The results, shown in Figure 3a reveal clustering of odors. For any individual odor, one can also obtain clustering of concentrations, when looking at each odor separately (not shown here).

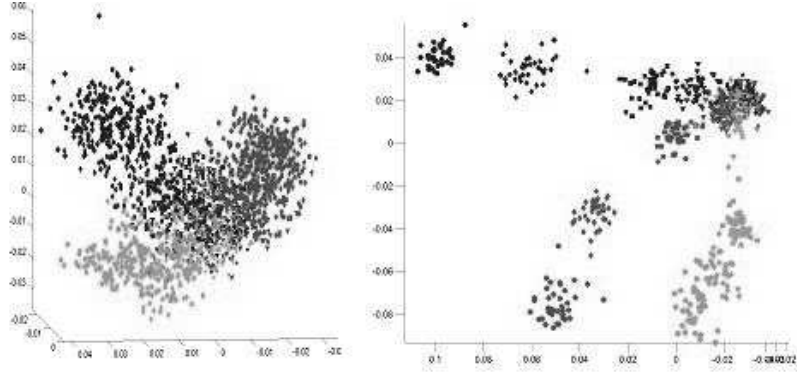


Fig. 3: 3-dimensional SVD reduction of local spatiotemporal data. 3 different shades specify the three odors. Left: Constant noisy odor applied for 1 sec. Right: Noisy non-odor input for 1 sec, followed by constant noisy odor for 1 sec, after which the odor decays for the next 3 secs. 15 trials were presented in bins of 100msec, leading to  $225 \times 50$  data points in 100 dimensions.

### 3.3 Spatial Analysis (*Firing Rates*)

Our third SVD experiment is to analyze the spike count data, i.e. we take the  $225 \times 2000$  matrix of data described above, and sum all columns (temporal-bins) together into 100 dimensional vectors, thus leading to a  $225 \times 100$  data matrix. The resulting clustering properties were similar in quality to those of Figure 2. Hence we conclude that the responses to different odors and different concentrations can be distinguished by total spike counts, i.e. the information is also carried by a rate code.

All these simulations were carried out under the assumption that the system is subjected to a constant odor throughout the numerical experiment. To check ourselves with respect to the experimental results of (5) we proceed to define a second set of numerical experiments, where a constant odor (with small noise) was turned on after one second of background activity, applied for one second and followed by three seconds of odor decay back to background activity. The results are that the spatiotemporal patterns retain the power to cluster different odors and concentrations, and so does the spike count analysis. In the local spatiotemporal analysis, the clustering results improved significantly for most time bins, as demonstrated in Figure 3b.

## 4 Discussion

We have obtained the desired odor and concentration clusters on all three levels of data analysis. Of particular importance is the fact that odors and concentrations clustered correctly for the local spatiotemporal analysis, which seems to be the most relevant to the biological system (inputs of Kenyon cells). In the recent experimental analysis of (5), the authors have demonstrated a representation of odors as manifolds with concentration as trajectories delineated by the temporal order of the local spatiotemporal data. We have obtained clusters for the different concentrations, but have not found clear trajectories within these clusters. We continue to investigate this point. We note that the DNF, with its one time-step dynamics, lacks a second, longer time-scale dynamics of the kind observed in the firing patterns of PNs of the Locust. This second time-scale may be responsible for some short-term memory that carries the odor information after it is being removed, leading also to the temporal-ordered trajectories mentioned above. We believe that adding suitable inertial characteristics to the DNF will allow our model to reproduce concentration-trajectories in place of the concentration clusters in the local spatiotemporal analysis.

### *Acknowledgment*

We wish to thank Vivek Jayaraman and Mark Stopfer for helpful discussions of their data and Gilles Laurent for the hospitality extended to one of us (OK).

## References

- [1] R. W. Friedrich and G. Laurent, 2001. Dynamic optimization of odor representations by slow temporal patterning of mitral cell activity. *Science* 291, 889-894.
- [2] D. Horn, B. Quenet, G. Dror, O. Kliper, 2003. Modeling Neural Spatiotemporal Behavior. *Neurocomputing*, 52-54 (proceedings of CNS02), 799-804.
- [3] B. Quenet and D. Horn, 2003. The Dynamic Neural Filter: A Binary Model of Spatiotemporal Coding. *Neural Computation* 15, 309-329.
- [4] J.P. Rospars, P. Lansky, P. Duchamp-Viret, A. Duchamp, 2000. Spiking frequency versus odorant concentration in olfactory receptor neurons. *BioSystems* 58, 133-141.
- [5] M. Stopfer, V. Jayaraman and G. Laurent. 2003. Intensity versus Identity Coding in an Olfactory System. *Neuron*, 39(6), 991-1004.
- [6] M. Wehr and G. Laurent, 1996. Odour encoding by temporal sequences of firing in oscillating neural assemblies. *Nature* 384, 162-166.